



# Activation of Nrf2 Is Required for Normal and ChREBP $\alpha$ -Augmented Glucose-Stimulated $\beta$ -Cell Proliferation

Anil Kumar,<sup>1</sup> Liora S. Katz,<sup>1</sup> Anna M. Schulz,<sup>2</sup> Misung Kim,<sup>3</sup> Lee B. Honig,<sup>1</sup> Lucy Li,<sup>1</sup> Bennett Davenport,<sup>1</sup> Dirk Homann,<sup>1</sup> Adolfo Garcia-Ocaña,<sup>1</sup> Mark A. Herman,<sup>4</sup> Cole M. Haynes,<sup>5</sup> Jerry E. Chipuk,<sup>1,2</sup> and Donald K. Scott<sup>1</sup>

*Diabetes* 2018;67:1561–1575 | <https://doi.org/10.2337/db17-0943>

**Patients with both major forms of diabetes would benefit from therapies that increase  $\beta$ -cell mass. Glucose, a natural mitogen, drives adaptive expansion of  $\beta$ -cell mass by promoting  $\beta$ -cell proliferation. We previously demonstrated that a carbohydrate response element-binding protein (ChREBP $\alpha$ ) is required for glucose-stimulated  $\beta$ -cell proliferation and that overexpression of ChREBP $\alpha$  amplifies the proliferative effect of glucose. Here we found that ChREBP $\alpha$  reprogrammed anabolic metabolism to promote proliferation. ChREBP $\alpha$  increased mitochondrial biogenesis, oxygen consumption rates, and ATP production. Proliferation augmentation by ChREBP $\alpha$  required the presence of ChREBP $\beta$ . ChREBP $\alpha$  increased the expression and activity of Nrf2, initiating antioxidant and mitochondrial biogenic programs. The induction of Nrf2 was required for ChREBP $\alpha$ -mediated mitochondrial biogenesis and for glucose-stimulated and ChREBP $\alpha$ -augmented  $\beta$ -cell proliferation. Overexpression of Nrf2 was sufficient to drive human  $\beta$ -cell proliferation *in vitro*; this confirms the importance of this pathway. Our results reveal a novel pathway necessary for  $\beta$ -cell proliferation that may be exploited for therapeutic  $\beta$ -cell regeneration.**

Patients with both major forms of diabetes suffer from insufficient functional pancreatic  $\beta$ -cell mass, making

therapies that expand  $\beta$ -cell mass a targeted goal of diabetes research (1). Furthermore, glucose is an important natural mitogen of  $\beta$ -cells both *in vitro* and *in vivo* (2–5). Glucose acts as a systemic driver of  $\beta$ -cell mass in response to increased insulin demand. Glucose metabolism triggers insulin secretion but also serves as a mechanism to signal cell proliferation. Thus, glucose-stimulated  $\beta$ -cell proliferation is an essential component of adaptive  $\beta$ -cell expansion and long-term glucose homeostasis (5). Human  $\beta$ -cells proliferate at much slower rates than rodent  $\beta$ -cells (1,6). Nonetheless, glucose metabolism drives human  $\beta$ -cell proliferation both *in vitro* and *in vivo* (4,7). Thus, understanding mechanisms of glucose-stimulated  $\beta$ -cell proliferation provides opportunities to develop therapies to expand  $\beta$ -cell mass.

We demonstrated that carbohydrate response element-binding protein (ChREBP $\alpha$ , gene symbol *MLXIPL*) is required for glucose-stimulated proliferation of rodent and human  $\beta$ -cells (4). Important for this study, overexpression of ChREBP $\alpha$  augments glucose-stimulated proliferation of both rodent and human  $\beta$ -cells. ChREBP $\alpha$  is a transcription factor that is activated by increased glucose metabolism and binds to carbohydrate response elements in order to drive the expression of target genes (8). Numerous posttranslational events modify the cellular

<sup>1</sup>Diabetes, Obesity, and Metabolism Institute, Icahn School of Medicine at Mount Sinai, New York, NY

<sup>2</sup>Departments of Oncological Sciences and Dermatology, Icahn School of Medicine at Mount Sinai, New York, NY

<sup>3</sup>Division of Endocrinology and Metabolism, Beth Israel Deaconess Medical Center, Harvard Medical School, Boston, MA

<sup>4</sup>Division of Endocrinology and Metabolism and Duke Molecular Physiology Institute, Duke University Medical Center, Durham, NC

<sup>5</sup>Cell Biology Program, Memorial Sloan Kettering Cancer Center, New York, NY

Corresponding author: Donald K. Scott, [donald.scott@mssm.edu](mailto:donald.scott@mssm.edu).

Received 9 August 2017 and accepted 5 May 2018.

This article contains Supplementary Data online at <http://diabetes.diabetesjournals.org/lookup/suppl/doi:10.2337/db17-0943/-/DC1>.

A.K. is currently affiliated with the Metabolic Phenotyping Core, University of Utah, Salt Lake City, UT.

A.M.S. is currently affiliated with the Division of Animal Physiology and Immunology, School of Life Sciences Weihenstephan, Technical University of Munich, Freising, Germany.

B.D. is currently affiliated with the Department of Immunology and Microbiology, University of Colorado Denver, Anschutz Medical Campus, Aurora, CO.

C.M.H. is currently affiliated with the Department of Molecular, Cell and Cancer Biology, University of Massachusetts Medical School, Worcester, MA.

© 2018 by the American Diabetes Association. Readers may use this article as long as the work is properly cited, the use is educational and not for profit, and the work is not altered. More information is available at <http://www.diabetesjournals.org/content/licence>.

localization, DNA binding activity, and transactivation activity of ChREBP $\alpha$ , making it an effective transcriptional sensor of increased glucose flux (9). ChREBP exists as two major isoforms (10). ChREBP $\alpha$  is the “classic” full-length, glucose-regulated form. ChREBP $\beta$  is an alternatively spliced isoform that lacks the low glucose inhibitory domain (which also contains nuclear export signals) and is unrestrained by low glucose, is constitutively nuclear, and is much more potent than its longer counterpart (Supplementary Fig. 1). ChREBP $\beta$  is induced by a carbohydrate response element (ChoRE) located near the start site of an alternative promoter for ChREBP $\beta$ . Thus induction of the  $\beta$  isoform leads to an autoregulated feed-forward loop: the newly synthesized ChREBP $\beta$  binds to the ChoRE on its own promoter (and other ChREBP target genes), leading to production of still more ChREBP $\beta$ . We recently found that the induction of ChREBP $\beta$ , from a nearly undetectable amount to a level comparable to that of ChREBP $\alpha$ , is required for glucose-stimulated proliferation (11). However, expression of ChREBP $\beta$  for too long and at too high a level, as may happen in response to diabetic hyperglycemia or through overexpression, results in  $\beta$ -cell death (12). By contrast, inducible overexpression of the full-length form of ChREBP (ChREBP $\alpha$ ) does not induce cell death and has no effect on glucose-stimulated insulin secretion (GSIS) (13) (see Supplementary Data). It is remarkable that overexpression of ChREBP $\alpha$  amplifies glucose-stimulated  $\beta$ -cell replication rates, without increasing apoptosis, in both rodent and human  $\beta$ -cells (4) (see RESULTS). This study was conducted to gain clarity on how ChREBP $\alpha$  augments glucose-stimulated proliferation of  $\beta$  cells.

The transcription factor nuclear factor erythroid 2-like 2 (Nrf2) mediates the expression of antioxidant enzyme genes and genes involved in intermediary metabolism, as well as mitochondrial biogenesis, acting through antioxidant response elements (AREs) (14). The antioxidant Nrf2 pathway has antiobesity and antidiabetic properties; it suppresses body weight gain when a high-calorie diet is consumed, increases plasma levels of fibroblast growth factor 21 in rodent models of obesity, and protects against diabetes complications (for a review, see [15]). Indeed, several Nrf2 activators have been under investigation in clinical trials for the treatment of diabetes (16).

In this study we demonstrate that ChREBP $\alpha$  initiates anabolic metabolism and increases mitochondrial mass and activity, at least in part, through activation of the Nrf2 pathway, thus augmenting glucose-stimulated  $\beta$ -cell proliferation. This process requires the induction of ChREBP $\beta$ . In addition, we show—to our knowledge for the first time—that activation of Nrf2 is necessary for glucose-stimulated proliferation of rodent and human  $\beta$ -cells and that overexpression of Nrf2 is sufficient to drive human  $\beta$ -cell proliferation.

## RESEARCH DESIGN AND METHODS

### Antibodies and Reagents

Antibodies for PGC1 $\alpha$ , PGC1 $\beta$ , and Nrf2 were purchased from Santa Cruz Biotechnology (Dallas, TX). Antibodies

for Nrf1 and BrdU were purchased from Abcam (Cambridge, MA). The ChREBP antibody (COOH-terminal) was obtained from Novus Biologicals (Littleton, CO). Antibodies to  $\beta$ -actin and Flag were obtained from Sigma-Aldrich (St. Louis, MO). The baculovirus expressing mitochondrial red fluorescent protein (CellLight Mitochondria-RFP, BacMam 2.0), DAPI, and all the Alexa fluorophore-tagged secondary antibodies were purchased from Life Technologies (Carlsbad, CA). Human Keap1 adenovirus was obtained from Vigene Biosciences, Inc. (Rockville, MD).

### Mice and Mouse Islet Isolation

A conditional targeting vector was produced through standard recombineering methods, with insertion of a *loxP* site 160 base pairs upstream from ChREBP exon 1b and a *loxP*, *frt*-flanked neo cassette 680 base pairs downstream from exon 1b. Germline-competent 129 W4 embryonic stem cells were transfected with the linearized targeting vector and screened through the use of long-range PCR. Two positive clones were expanded and injected into C57Bl/6J blastocysts to obtain chimeric mice (generated in the Transgenic Core Facility at Beth Israel Deaconess Medical Center). Chimeric mice were crossed with C57Bl/6J mice to generate offspring and to confirm germline transmission of the floxed ChREBP exon 1b. Mice carrying the floxed allele were crossed with mice expressing Flp1 recombinase (stock no. 003800; The Jackson Laboratory, Bar Harbor, ME) to remove the *frt*-flanked neo cassette. Mouse islets were isolated and cultured as previously described (4).

### Cell Culture and Adenovirus

INS1-derived 832/13 cells (henceforth referred to as INS1 cells) (17) were cultured as described previously (18). The proliferation assay, incorporating BrdU, was carried out with INS1 cells, as previously described (11). Islets were dispersed and cultured as previously described (4). Cells were transduced as previously described (4): transduction with serum-free RPMI medium containing 150–300 multiplicity of infection adenovirus for 2 h, with the adenoviral vectors encoding Flag-tagged wild-type ChREBP $\alpha$  (Ad.ChREBP $\alpha$ ), Keap1 (Ad.Keap1), Nrf2 (Ad.Nrf2), and Cre (Ad.Cre), or either green fluorescent protein (GFP) (Ad.GFP) or LacZ (Ad.LacZ) adenovirus, used as controls. Adenoviral transduction lasted for 48 h before glucose treatment unless stated otherwise. To knock down Nrf2, cells transduced with Ad.LacZ or Ad.ChREBP $\alpha$  were transfected with rat Nrf2 small interfering RNA (siRNA) (catalog no. AM16708; Ambion). The Ad.Cherry-ChREBP $\beta$  adenovirus was made using the Gateway recombination system (Life Technologies) after subcloning a truncated mouse ChREBP cDNA (nucleotides 531–2,595) with Cherry cDNA in frame on the N-terminus into the pENTR vector, as described previously (1). Nrf2- and Keap1-expressing adenoviruses were purchased from Vector Biolabs.

### Cell Proliferation

INS1 cells were cultured on LabTek II chamber slides (Nunc, Rochester, NY). BrdU (10  $\mu$ g/mL) was added during

the last 40 min of incubation, and cells were fixed in 2% paraformaldehyde in PBS. Cells were immunostained using rat anti-BrdU antibody and Alexa594-labeled antirat antibody. Nuclei were stained with DAPI. Cells were imaged with a Zeiss Axioplan 2 microscope or either a Zeiss LSM510 or a Zeiss LSM880 confocal microscope. Proliferation in dispersed human islet cells was determined by Ki67 staining (11).

### Immunofluorescent Staining

INS1 cells were cultured on cell culture–treated Corning BioCoat coverslips (catalog no. 354087), and immunofluorescent staining and imaging were carried out as described above (11).

### Human Islets

Human cadaveric islets received from the Integrated Islet Distribution Program were cultured as previously described (4). To knock down Nrf2 in human islet cells, dispersed human islet cells were transfected with a pooled Accell siRNA targeting Nrf2 (catalog no. E-003755–00; Dharmacon) through the use of a previously described method (4).

### RT-PCR and Quantitative Real-time PCR

Total RNA was extracted and RT-PCR was performed as previously described (4). To measure mitochondrial DNA in INS1 cells, DNA was extracted using a Wizard Genomic DNA Purification Kit (Promega, Madison, WI). The sequences of primers used are listed in Supplementary Table 1.

### Immunoblotting

Protein extracts were prepared and immunoblotted as previously described (19).

### Determination of Mitochondrial Content

INS1 cells were cotransduced with CellLight Mitochondria-RFP baculovirus and either Ad.LacZ or Ad.ChREBP $\alpha$  for 48 h, then were treated with the indicated glucose concentrations for 20 h. Dispersed human islet cells were treated with Ad.LacZ or Ad.ChREBP $\alpha$  and stained with MitoTracker Red CMXRos and immunostained for insulin. A TMRE-Mitochondrial Membrane Potential Assay Kit was obtained from Abcam. The antibody to Keap1 was obtained from Cell Signaling Technology (Danvers, MA). To measure mitochondrial DNA content, we used 100 ng DNA and primers to the D-loop region of the mitochondrial genome. GAPDH primers were used to normalize mitochondrial DNA abundance to genomic DNA abundance.

### Determination of ATP Content and ATP-to-ADP Ratios

To determine ATP content, cell extracts were passed through a filter (molecular weight cutoff 10 kDa), and the ATP content in the filtrate was determined using the ENLITEN ATP Assay System (Promega). ATP and ADP levels were determined using a kit (catalog no. ab65313; Abcam), according to the manufacturer's instructions.

### Determination of Autophagy, Reactive Oxygen Species, and Cell Death

INS1 cells were transduced with 150 multiplicity of infection of the indicated adenovirus for 48 h total. Glucose

concentrations were changed before the last 16 h of culture. CYTO-ID Green (Enzo Life Sciences) was then added at 37°C for 25 min. Nuclei were stained with NucBlue (Molecular Probes), and cells were imaged with a Zeiss Observer Z1 microscope. Autophagy was quantified using a FACSCalibur flow cytometer (BD Biosciences). Reactive oxygen species (ROS) levels were determined using a kit (catalog no. CM-H2DCFDA; Thermo Fisher Scientific) according to the manufacturer's recommendations. TUNEL was assessed using the DeadEND Fluorometric TUNEL System (Promega). Cells were fixed and were stained for TUNEL and insulin (A056401; Dako), and nuclei were identified with DAPI.

### ARE-Luciferase Assay

INS1 cells were transfected with a pGL4.37-luc2p/ARE/Hygro vector (Promega), and a pSV-galactosidase control vector, 24 h after transduction with Ad.ChREBP $\alpha$ . Following experimental incubation, luciferase activity was determined as previously described (11), and the values were normalized to  $\beta$ -galactosidase activity using a galactosidase assay kit from Promega.

### Measurement of Oxygen Consumption Rate

INS1 cells were transduced with Ad.LacZ or Ad.ChREBP $\alpha$  and after 48 h the oxygen consumption rate (OCR) was determined in a Seahorse XFe96 extracellular flux analyzer. Basal OCR was determined, and OCRs were recorded after the following additions: oligomycin (2.5  $\mu$ mol/L), carbonyl cyanide 4-(trifluoromethoxy) phenylhydrazone (FCCP; 1  $\mu$ mol/L), and rotenone (1  $\mu$ mol/L) and antimycin A (1  $\mu$ mol/L).

### Metabolomics

For metabolomic studies, cell pellets were submitted for liquid chromatography–mass spectrometry module 3 metabolite profiling at the Stable Isotope & Metabolomics Core (Albert Einstein School of Medicine, Bronx, NY), which was done as previously described (20).

### GSIS

Insulin secretion in response to 5.5 and 20 mmol/L glucose was measured in human islets transduced with Ad.LacZ and Ad.ChREBP $\alpha$  through the use of a previously described method (21).

### Statistics

All the data shown are the mean  $\pm$  SE of results of a number of experiments (indicated in the figure legends). Significance was determined by the unpaired two-way *t* test and one-way ANOVA with the post hoc Tukey honestly significant difference test. Differences were considered significant if the *P* value was  $<0.05$ .

## RESULTS

### ChREBP $\alpha$ Reprograms Metabolism and Promotes Mitochondrial Biogenesis

Some controversy exists in the literature about the role of ChREBP in  $\beta$ -cells. Several studies suggested that ChREBP is at least partially responsible for glucose toxicity (12,22–24). Thus, we were initially surprised that ChREBP $\alpha$

overexpression augments glucose-stimulated  $\beta$ -cell proliferation without apparent cytotoxicity (4). We believe that this can be explained by the recent discovery of ChREBP $\beta$ , an alternatively spliced isoform that lacks the low glucose inhibitory domain and nuclear export signals, is constitutively nuclear, and is constitutively and potently active (10) (Supplementary Fig. 1). ChREBP $\beta$  is induced by a ChoRE. Thus induction of the  $\beta$  isoform initiates an autoregulated feed-forward loop. We recently demonstrated that induction of ChREBP $\beta$  is necessary for glucose-stimulated proliferation of rat  $\beta$ -cells (11). However, apoptosis results when ChREBP $\beta$  is overexpressed in  $\beta$ -cells at a level that is many fold higher than physiological levels (12) (Supplementary Fig. 2). Together, these observations suggest that physiological induction of the potent ChREBP $\beta$  isoform is necessary for adaptive  $\beta$ -cell expansion, but that too much for too long, as may happen from prolonged hyperglycemia in diabetes, or through overexpression with viral vectors, is harmful to  $\beta$ -cells. By contrast, ChREBP $\alpha$  overexpression in INS1 cells or human islets does not stimulate endoplasmic reticulum stress, result in apoptosis, alter ATP-to-ADP ratios, or affect GSIS (13) (Supplementary Fig. 2), but it does amplify glucose-stimulated  $\beta$ -cell proliferation (4).

To place the effects of ChREBP $\alpha$  in context with what we know about ChREBP $\beta$ , we tested whether ChREBP $\beta$  is required for ChREBP $\alpha$  overexpression to have an effect. Islets were isolated from floxed ChREBP $\beta$  mice, were treated with Ad.ChREBP $\alpha$  or Ad.GFP as a control, and were cotreated with Ad.Cre recombinase or a control (Supplementary Fig. 3). Treatment with Cre effectively removed exon 1b, depleting ChREBP $\beta$  while allowing ChREBP $\alpha$  to be expressed. Control islets cultured in 20 mmol/L glucose displayed increased proliferation in insulin-positive cells, an effect that was significantly diminished after depletion of ChREBP $\beta$ , in accordance with our previous findings (11). As expected, islets transduced with the ChREBP $\alpha$  adenovirus exhibited amplification of glucose-stimulated  $\beta$ -cell proliferation. When islets were treated with both Ad.ChREBP $\alpha$  and Ad.Cre, proliferation was reduced to basal levels. It is interesting to note that treatment with ChREBP $\alpha$ , which increased ChREBP $\alpha$  levels many fold (Fig. 1), only increased ChREBP $\beta$  levels by  $\sim$ 80% and did not increase levels of several known ChREBP target genes including *Pklr*, *Glut2*, and *Txnip* (Supplementary Fig. 2). Thus the effects of ChREBP $\alpha$  on glucose-stimulated  $\beta$ -cell proliferation require ChREBP $\beta$  without hyperactivation of ChREBP target genes. These results suggest that other signaling pathways must be involved in the augmentation of proliferation when ChREBP $\alpha$  is overexpressed.

Because all proliferating cells require metabolic reprogramming (25), we examined how ChREBP $\alpha$  affects intermediary metabolism. INS1 cells (17) were transduced with a control adenovirus, or one expressing ChREBP $\alpha$ , and cultured in 2 or 20 mmol/L glucose. A metabolomic analysis was performed, the results of which are shown in Fig. 1A and Supplementary Table 2. As expected, we found

that 20 mmol/L glucose increased the abundance of glycolytic products including glucose-6-phosphate, fructose 1, 6-bisphosphate, glycerol-3-phosphate, pyruvate, and lactate. It is remarkable that ChREBP $\alpha$  treatment further increased their levels. In a similar way, 20 mmol/L glucose increased amounts of the pentose phosphate pathway intermediates 6-phospho-D-gluconate and ribose-5-phosphate, and ChREBP $\alpha$  increased them further. In addition, the same pattern was seen with the tricarboxylic acid (TCA) cycle intermediates succinate, fumarate, and malate. Furthermore, whereas aspartate levels were not increased by glucose alone, aspartate increased after treatment with ChREBP $\alpha$  and both low and high glucose (Fig. 1A and Supplementary Table 2). Many of the metabolites in these pathways increased significantly with ChREBP $\alpha$  treatment, even in 2 mmol/L glucose (Supplementary Table 2), suggesting increased anaplerotic flux. The increased TCA cycle intermediates suggest an increase in mitochondrial activity. Accordingly, in ChREBP $\alpha$ -treated cells in 2 mmol/L glucose we found a significant increase in ATP (Fig. 1B) that was equivalent to that of control cells in 20 mmol/L glucose; however, we found no change in ATP-to-ADP ratios (Supplementary Fig. 2). These collective results demonstrate that ChREBP $\alpha$  increases the glycolytic pentose pathway and TCA cycle intermediates, with a high capacity to generate ATP—a metabolic signature of proliferating cells (25,26).

To explore further the effect of ChREBP $\alpha$  on mitochondria, we measured mitochondrial DNA content and found that it significantly increased in response to glucose. Treatment with ChREBP $\alpha$  increased mitochondrial DNA in both low and high glucose (Fig. 1C). Mitochondria were initially visualized by cotransducing a baculovirus expressing mitochondria-targeted red fluorescent protein with either Ad.LacZ or Ad.ChREBP $\alpha$  in INS1 cells.; images of fluorescent cells were acquired by confocal microscopy (Fig. 1D and Supplementary Fig. 4A). Mitochondria appeared as small rods in control cells treated with high glucose. By contrast, mitochondria in ChREBP $\alpha$ -treated cells were tubular and fluoresced brightly. The fluorescent signal intensity in ChREBP $\alpha$ -treated cells was approximately twofold higher than that in control cells (Fig. 1D and E). Flow cytometric analysis provided similar results (Supplementary Fig. 4B).

To test whether ChREBP $\alpha$  affects mitochondrial function, we stained INS1 cells with tetramethylrhodamine ethyl ester (TMRE) as a measure of mitochondrial transmembrane potential ( $\Delta\Psi$ M) (27). ChREBP $\alpha$  significantly increased  $\Delta\Psi$ M in INS1 cells (Fig. 2A and B). ChREBP $\alpha$ -treated cells displayed larger, more elongated mitochondria. In addition, when cells preloaded with TMRE were treated with FCCP, a proton ionophore that depolarizes the mitochondrial membrane (27), the loss of the TMRE label was significantly and proportionately reduced in both LacZ- and ChREBP $\alpha$ -treated cells (Fig. 2B). Thus ChREBP $\alpha$ -treated cells have more mitochondrial content with increased  $\Delta\Psi$ M than do control cells.

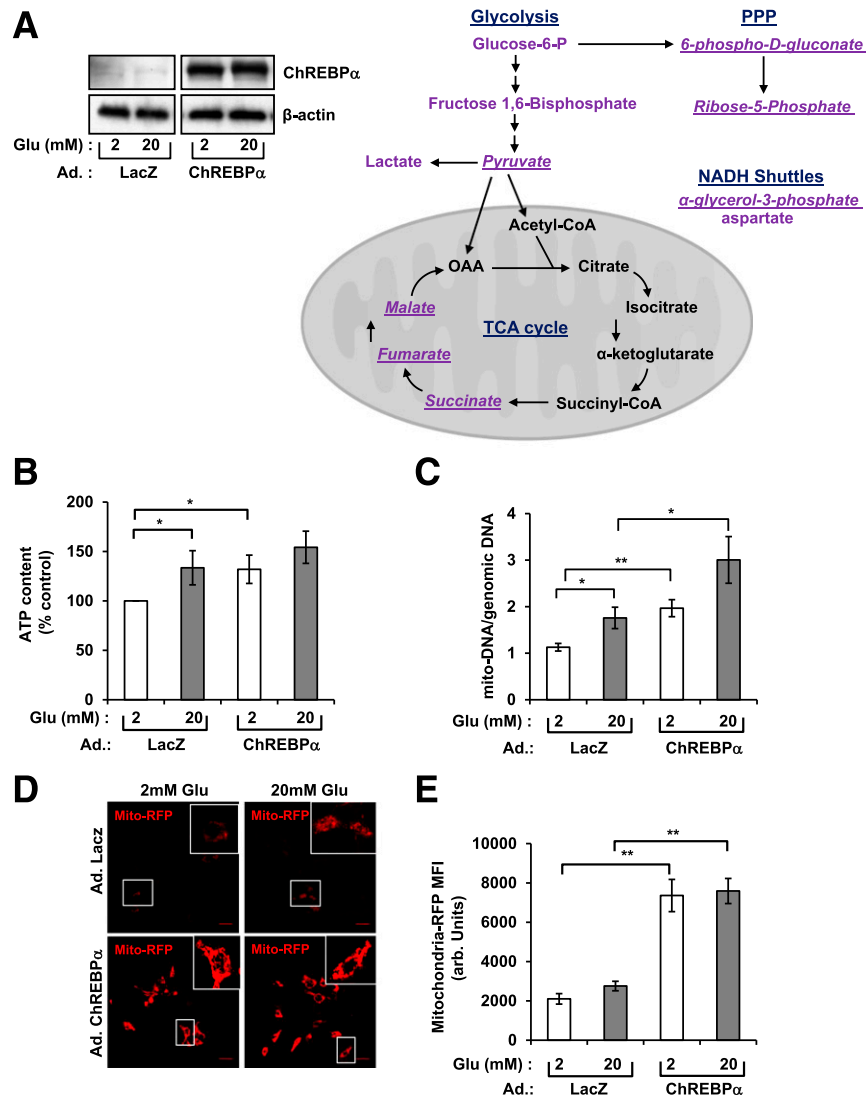


**Figure 1**—ChREBP $\alpha$  increases anabolic metabolites and  $\beta$ -cell mitochondrial content. **A:** INS1 cells were treated with Ad.ChREBP $\alpha$  or Ad.LacZ (for 48 h) and 2 or 20 mmol/L glucose (Glu) (for 20 h), and cell extracts were prepared for immunoblotting (left; lanes shown are from the same blot with the same exposure) and metabolomic analysis (see also Supplementary Table 2). The schema to the right represents the metabolites (purple) that were significantly increased in response to ChREBP $\alpha$ . Metabolites underlined and in italics were increased even in low glucose. OAA, oxaloacetate; PPP, pentose phosphate pathway. **B:** Total intracellular ATP content from INS1 cells was determined and normalized to protein content; values are shown as a percentage of the control (stimulated with 2 mmol/L glucose and treated with Ad.LacZ). **C:** Mitochondrial DNA (mito-DNA) content was determined from INS1 cells through the use of quantitative real-time PCR and normalized to genomic DNA content. **D:** INS1 cells were cotransduced with a baculovirus expressing mitochondria-targeted red fluorescent protein (Mito-RFP) with either Ad.LacZ or Ad.ChREBP $\alpha$  and were treated as indicated. Scale bars = 10  $\mu$ m. **E:** Signal intensities from the images in **D** relative to the control (treated with low glucose). The values shown are the mean  $\pm$  SE ( $n = 3$ –5). \* $P < 0.05$ ; \*\* $P < 0.01$ . arb., arbitrary; MFI, mean fluorescence intensity.

To test the oxidative capacity of mitochondria, we measured the OCR. ChREBP $\alpha$  significantly enhanced basal and maximal respiratory capacity (FCCP-induced OCR), and OCR coupled to ATP synthesis (basal OCR – OCR uncoupled by oligomycin) (Fig. 2C–F). These findings were consistent with the increased ATP levels in ChREBP $\alpha$ -treated cells (Fig. 1B). It is notable that spare respiratory capacity (FCCP-induced OCR – basal OCR) in ChREBP $\alpha$ -treated cells was similar to that of control cells (Fig. 2G). Thus, the increased capacity for ATP generation was not associated with overt mitochondrial dysfunction (28).

To assess whether ChREBP $\alpha$  affects mitochondria in human  $\beta$ -cells, we labeled dispersed human islet cells with MitoTracker Red CMXRos, whose accumulation is dependent on membrane potential (29), and an antibody against insulin (Fig. 3A and Supplementary Fig. 5). Remarkably, glucose increased the MitoTracker signal in human  $\beta$ -cells, and ChREBP $\alpha$  increased it further (Fig. 3A and B and Supplementary Fig. 5). In addition, ATP levels were increased by glucose in control cells, and in ChREBP $\alpha$ -treated human islets in low glucose (Fig. 3C). These data collectively demonstrate that ChREBP $\alpha$  increases

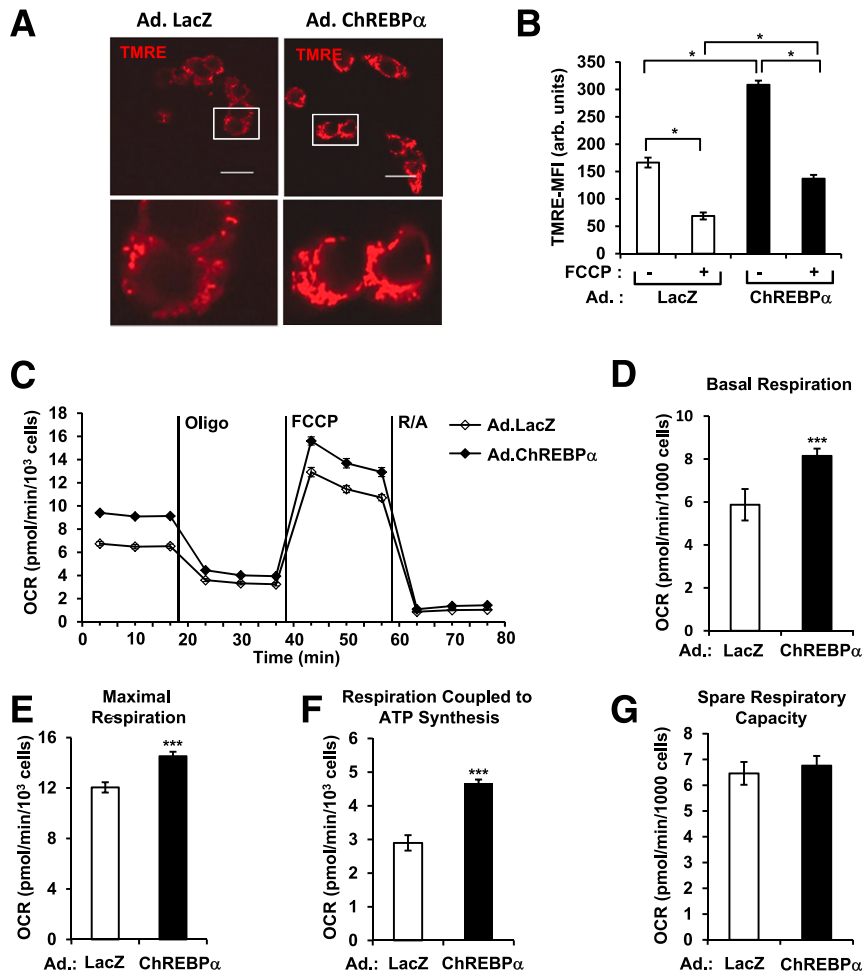


**Figure 2**—ChREBP $\alpha$  enhances mitochondrial oxidative metabolism. **A:** INS1 cells were treated as indicated and cultured in 11 mmol/L glucose. Mitochondrial membrane potential was determined by TMRE labeling and confocal microscopy. Scale bars = 14  $\mu$ m. **B:** The intensity of individual cells in images acquired by confocal microscopy (as shown in **A**) were quantified with ImageJ software. arb., arbitrary; MFI, mean fluorescence intensity. **C:** The OCR of INS1 cells cultured in 11 mmol/L glucose was measured using a Seahorse XFe96 analyzer. Oligo, oligomycin; R/A, rotenone and antimycin A. **D–G:** Graphs show basal respiration (**D**); maximal respiratory capacity (**E**) (calculated as the difference between FCCCP-induced OCR and OCR after addition of the R/A mixture; OCR by nonmitochondrial organelles); the difference between basal OCR and the oligomycin-insensitive OCR (**F**), which is the OCR coupled to ATP synthesis; and the spare respiratory capacity (**G**), calculated by subtracting basal OCR from FCCCP-induced OCR. The data shown are the mean  $\pm$  SE ( $n = 3$  or 4). \* $P < 0.05$ , \*\*\* $P < 0.001$ .

mitochondrial size and activity in both rodent and human  $\beta$ -cells.

### ChREBP $\alpha$ Activates the Antioxidant Nrf2 Pathway

To understand better the mechanism by which ChREBP $\alpha$  increases mitochondrial activity, we tested whether ChREBP $\alpha$  increased the expression of known mediators of mitochondrial activity and biogenesis. As shown in Supplementary Fig. 6, mRNA levels of PGC1 $\alpha$  were not changed. PGC1 $\beta$  mRNA levels were modestly increased, but ChREBP $\alpha$  had no effect on PGC1 $\beta$  protein levels. In addition, levels of Tfam, Polrmt, Tfb1m, Tfb2m, and Polg mRNA did not significantly change with ChREBP $\alpha$  treatment. Nrf2 is a master regulator of antioxidant pathways, and its activation is often associated with increased mitochondrial activity (14,15,30–32). ChREBP $\alpha$  substantially increased Nrf2 protein abundance in both 2 and 20 mmol/L

glucose (Fig. 4A and B), but it did not change mRNA levels (Supplementary Fig. 6), suggesting regulation at a post-translational level. Furthermore, Nrf2 abundance was clearly increased and was localized in the nucleus and cytoplasm after treatment with ChREBP $\alpha$ , as indicated by immunofluorescence (Fig. 4C). As shown in Fig. 4D, glucose increased ARE-driven luciferase activity in control cells, suggesting that activation of Nrf2 is a natural component of the glucose response in  $\beta$ -cells. ChREBP $\alpha$  enhanced ARE activity in both low and high glucose concentrations. We note that because Nrf2 abundance did not increase with glucose (Fig. 4B), there may be Nrf2-independent mechanisms through which glucose increases ARE activity. In addition, we found that ChREBP $\alpha$  upregulated the antioxidant enzymes H01 and Nq01, as well as the mitochondrial biogenic transcription factor Nrf1 (Fig. 4E). At the protein level, ChREBP $\alpha$  also increased

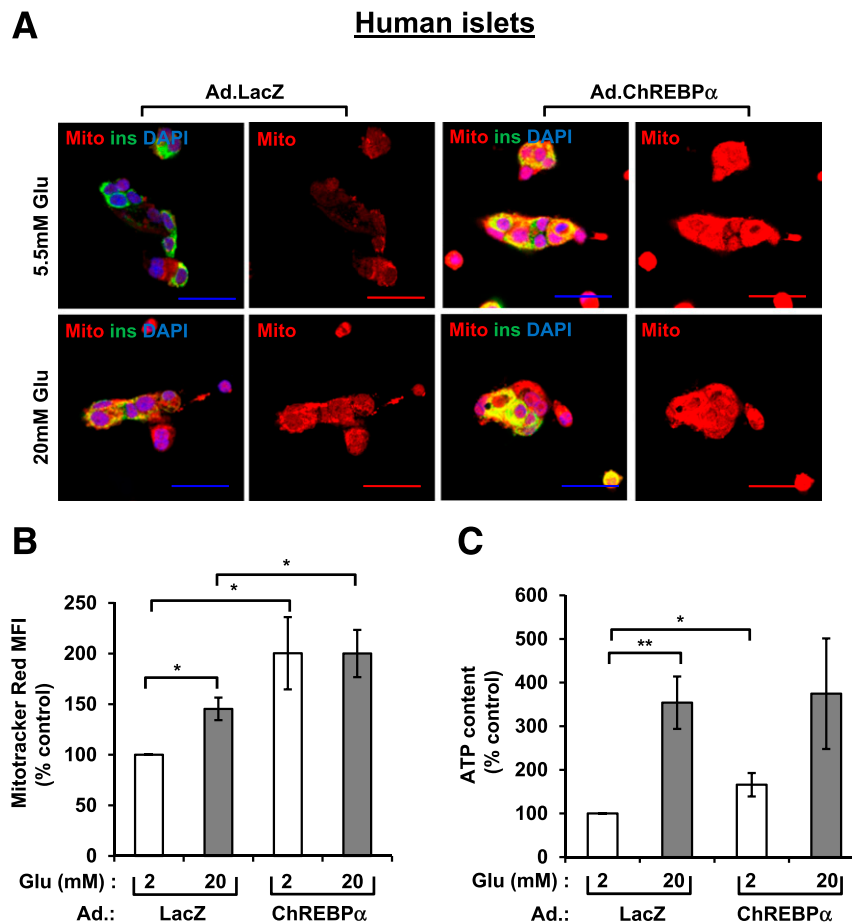


**Figure 3**—ChREBP $\alpha$  increases  $\beta$ -cell mitochondrial activity and ATP production in human islets. **A**: Dispersed human islets were transduced with the indicated adenovirus, treated as shown, and labeled with MitoTracker Red CMXRos (Mito) and an anti-insulin antibody (ins). Scale bars = 20  $\mu$ m. **B**: The mitochondrial signal intensity was determined from the images in **A** and is shown relative to the control (treated with low glucose [Glu]). **C**: Total intracellular ATP content was determined in human islets and normalized to protein content. Data are shown as a percentage of the control (stimulated with low Glu and treated with Ad.LacZ). The values shown are the mean  $\pm$  SE ( $n = 3$ –5). \* $P < 0.05$ , \*\* $P < 0.01$ . MFI, mean fluorescence intensity.

Nrf1, which contains an ARE and is downstream from Nrf2 (33) (Fig. 4F). Thus, ChREBP $\alpha$  activates the Nrf2 pathway.

#### Activation of Nrf2 Is Essential for Glucose-Stimulated $\beta$ -Cell Proliferation and for ChREBP $\alpha$ -Augmented Mitochondrial Biogenesis and Proliferation

To determine whether Nrf2 is required for glucose-stimulated  $\beta$ -cell proliferation or ChREBP $\alpha$ -mediated mitochondrial biogenesis, we first used an siRNA knockdown approach. Nrf2 abundance was modestly decreased by siRNA in INS1 cells (Fig. 5A). Depletion of Nrf2 blocked glucose-stimulated  $\beta$ -cell proliferation of INS1 cells under control conditions. In addition, decreasing Nrf2 inhibited ChREBP $\alpha$ -augmented glucose-stimulated proliferation (Fig. 5B). Furthermore, suppression of Nrf2 resulted in diminished mitochondrial membrane potential, as determined by TMRE labeling, both under control conditions and after treatment with ChREBP $\alpha$  (Fig. 5C and D).

To determine whether Nrf2 was required for human  $\beta$ -cell proliferation, human islet cells were treated with

pooled lipid-conjugated Accell siRNA, which knocks down genes in human islet cells without toxicity and preserves glucose-mediated proliferation (4). Treatment with Accell siRNA against Nrf2 resulted in a modest decrease in Nrf2 protein levels (Fig. 5E). Remarkably, depletion of Nrf2 in human  $\beta$ -cells diminished glucose-stimulated proliferation of both control cells and  $\beta$ -cells whose glucose response was augmented by ChREBP $\alpha$  treatment (Fig. 5E and F). Together, these experiments show for the first time that Nrf2 is necessary for normal glucose-stimulated proliferation and for ChREBP $\alpha$ -augmented glucose-stimulated proliferation of rodent and human  $\beta$ -cells.

Nrf2 is regulated by its interaction with Keap1, a substrate adaptor protein for a Cul3-containing E3 ligase that maintains Nrf2 at low levels through polyubiquitination and proteasomal degradation (34,35). To confirm the siRNA data, we transduced INS1 cells with an adenovirus expressing human Keap1. As expected, increased Keap1 was accompanied by a reduction of Nrf2 protein levels in both low and high glucose (Fig. 6A). Treatment with Keap1

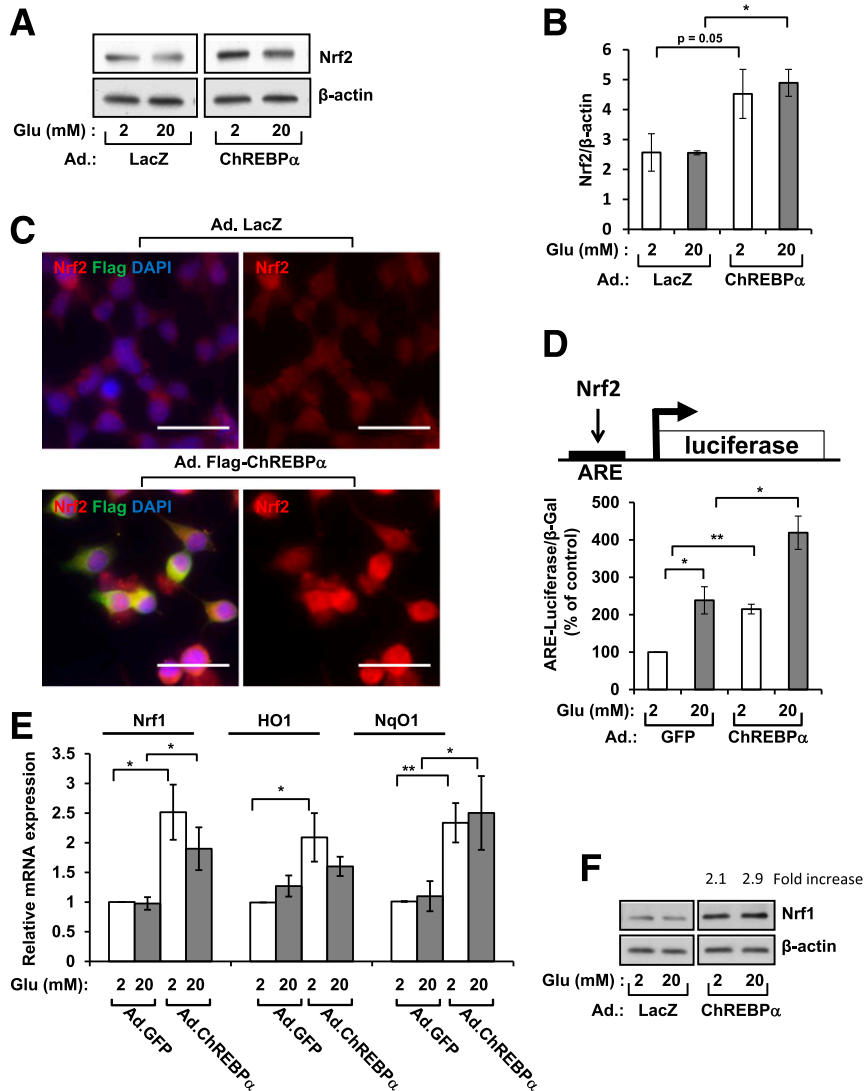


**Figure 4**—ChREBP $\alpha$  activates the Nrf2 pathway. *A*: Immunoblots of extracts from INS1 cells treated as shown. The lanes shown here are from noncontiguous lanes on the same blot with the same exposure. *B*: Quantification of densitometry from the immunoblots in *A*. *C*: INS1 cells cultured in 11 mmol/L glucose (Glu) were treated with the indicated adenovirus and were fixed and stained with antibodies against Nrf2 and Flag. Scale bars = 20  $\mu$ m. *D*: INS1 cells were treated as indicated, and luciferase activity was measured in cell extracts and normalized to  $\beta$ -galactose ( $\beta$ -Gal) activity. *E*: The abundance of mRNA relative to  $\beta$ -actin in the indicated genes was measured by RT-PCR. *F*: Immunoblots with antibodies against Nrf1 and actin. The noncontiguous lanes shown are from the same blot with the same exposure (see also Supplementary Fig. 6). Data are the mean  $\pm$  SE ( $n = 4$ ). \* $P < 0.05$ ; \*\* $P < 0.01$ .

reduced glucose-stimulated ARE-driven luciferase activity in Ad.GFP-treated control cells, consistent with its ability to diminish Nrf2 (Fig. 6B). In addition, cells overexpressing Keap1 exhibited poor TMRE labeling (Fig. 6C and D). Further, Keap1 decreased basal and glucose-stimulated proliferation of INS1 cells, as expected because of the decrease of Nrf2 (Fig. 6E). It is surprising that when cells were treated with both Keap1 and ChREBP $\alpha$ , the abundance of Keap1 decreased. Nrf2 abundance consequently increased to levels higher than those stimulated by ChREBP $\alpha$  (Fig. 6A). Keap1 had no significant effect on the ChREBP $\alpha$ -mediated increase in ARE activity (Fig. 6B). In addition, no Keap1-mediated loss in  $\Delta\Psi$ M occurred when ChREBP $\alpha$  was coexpressed with Keap1 (Fig. 6C and

D). Furthermore, ChREBP $\alpha$  rescued the Keap1-mediated inhibition of proliferation, presumably because Nrf2 downregulation was blocked. Together, these data suggest that overexpression of Keap1 inhibits Nrf2, consistent with the siRNA data presented above (Fig. 5). However, coexpression of ChREBP $\alpha$  and Keap1 led to decreased Keap1 levels and increased Nrf2 abundance, providing a possible explanation for how ChREBP $\alpha$  promotes the induction of Nrf2.

To determine whether these events were reflective of human  $\beta$ -cell biology, we treated human islet cells with Keap1 or with a combination of Keap1 and ChREBP $\alpha$  (Fig. 6F). In human  $\beta$ -cells, Keap1 decreased Nrf2 levels, as expected. Coexpression of ChREBP $\alpha$  reduced the abundance



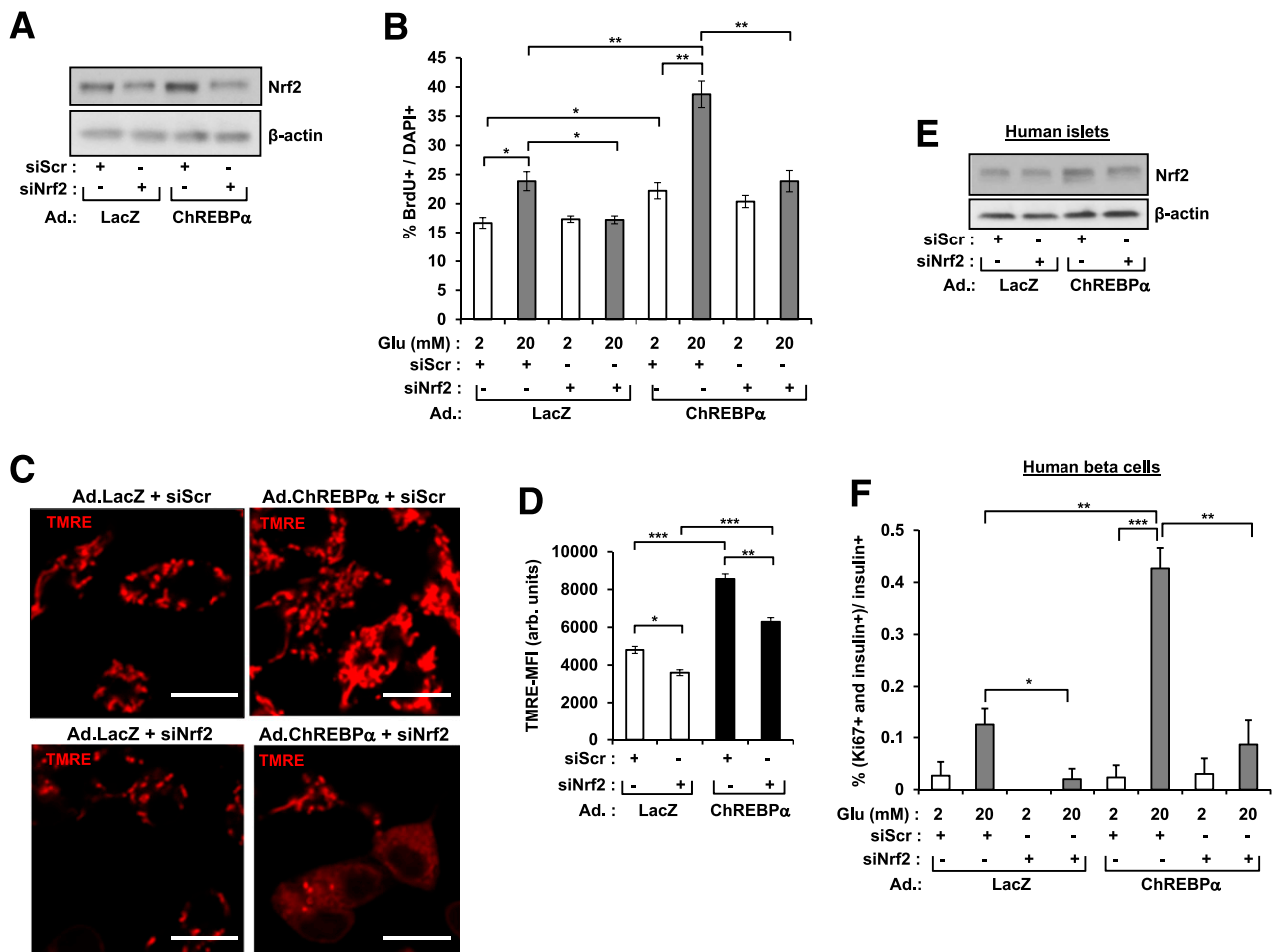


**Figure 5**—Knockdown of Nrf2 decreases mitochondrial activity and glucose (Glu)-stimulated  $\beta$ -cell proliferation. **A**: Immunoblots of extracts from INS1 cells cultured in 11 mmol/L Glu and treated with control siRNA or scrambled siRNA (siScr). Nrf2 was decreased  $\sim$ 30%, as determined by densitometry. **B**: Proliferation of INS1 cells was determined through the use of BrdU staining. **C**: INS1 cells were treated as indicated and were labeled with TMRE. Scale bars = 10  $\mu$ m. **D**: Results from the TMRE labeling (as shown in C) were quantified. **E**: Immunoblots of human islet extracts were treated as indicated. Nrf2 was decreased  $\sim$ 20% and  $\sim$ 30% in GFP- and ChREBP $\alpha$ -treated islets, respectively. **F**: Dispersed human cells were fixed and stained for insulin and Ki67. Results are the mean  $\pm$  SE ( $n = 3$ ) of the percentage of Ki67- and insulin-positive cells. \* $P < 0.05$ ; \*\* $P < 0.01$ ; \*\*\* $P < 0.001$ . arb., arbitrary; MFI, mean fluorescence intensity.

of Keap1 and maintained Nrf2 at levels comparable with those of the control. Furthermore, Keap1 treatment decreased MitoTracker Red CMXRos labeling in human  $\beta$ -cells, in accordance with diminished Nrf2 (Fig. 6G and H). However, Keap1 only slightly attenuated the dramatic increase in MitoTracker labeling that occurred after treatment with ChREBP $\alpha$ . In addition, Keap1 inhibited basal and glucose-stimulated  $\beta$ -cell proliferation in human islets (Fig. 6I), in agreement with the Nrf2 siRNA data (Fig. 5). It is important to note that coexpression with Keap1 and ChREBP $\alpha$  prevented this effect (Fig. 6I), in concert with the results shown in Fig. 5. Taken together, these data suggest that Nrf2 is essential for glucose-stimulated  $\beta$ -cell proliferation.

#### Overexpression of Nrf2 Is Sufficient to Drive Human $\beta$ -Cell Proliferation

To test whether overexpression of Nrf2 affects  $\beta$ -cell proliferation, we dispersed human islet cells and transduced

them with either control Ad.LacZ or Ad.Nrf2 (Fig. 7). Cells were cultured for 16 h with low glucose (2 or 6 mmol/L) or high glucose (20 mmol/L) and were fixed and immunostained for insulin and Ki67. As expected, 20 mmol/L glucose increased Ki67 staining in control cells by approximately twofold. It is surprising, however, that Nrf2 overexpression resulted in an approximately ninefold increase in human  $\beta$ -cells at the low glucose conditions and displayed a fourfold increase of proliferation with high glucose—equivalent to that in the control high-glucose group. These proliferative effects did not alter cell death, as shown in Supplementary Fig. 7. Thus, exogenous expression of Nrf2 is sufficient to drive human  $\beta$ -cell proliferation.

#### DISCUSSION

Here we show that activation of the Nrf2 pathway is required for normal and ChREBP $\alpha$ -enhanced glucose-stimulated

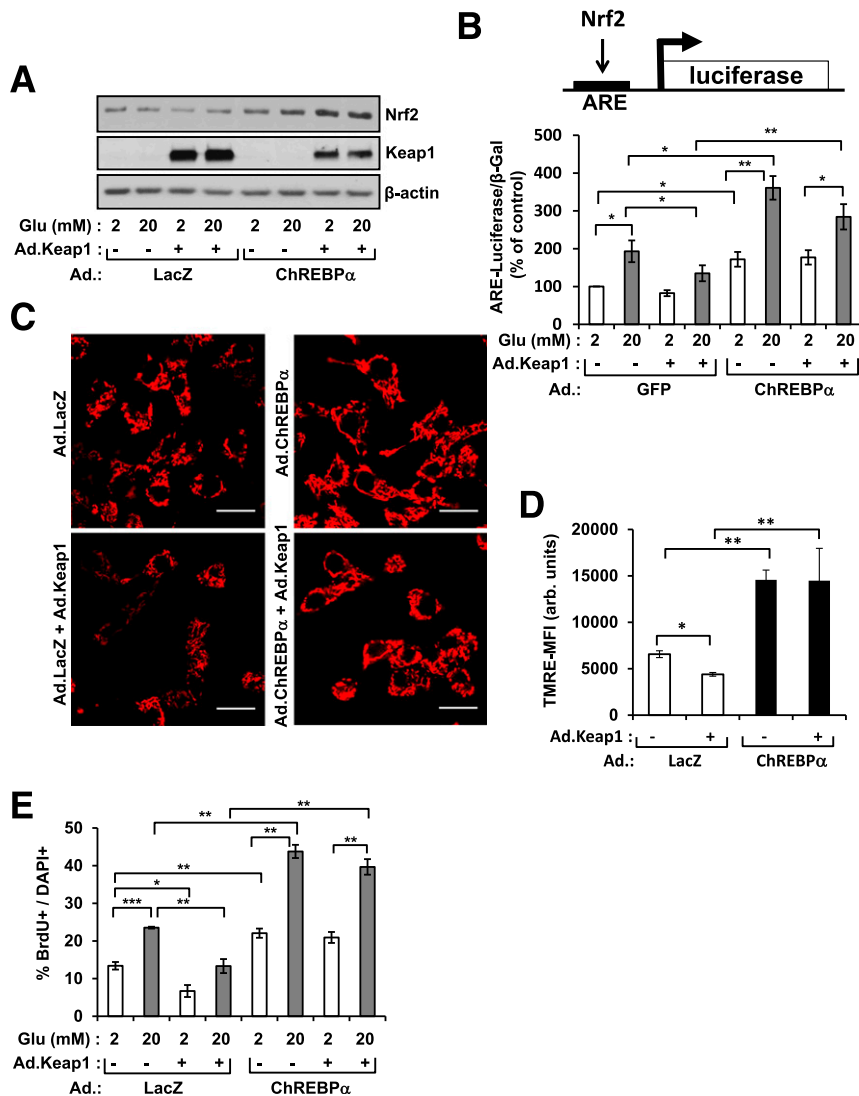


**Figure 6**—Keap1 decreases Nrf2, decreasing mitochondrial function and proliferation, whereas ChREBP $\alpha$  decreases Keap1, reversing the effects of Nrf2 depletion. **A**: Immunoblots from extracts of INS1 cells treated as indicated. **B**: INS1 cells were treated as shown, and luciferase activity was measured and normalized to  $\beta$ -galactosidase ( $\beta$ -Gal) activity (mean  $\pm$  SE).  $*P < 0.05$ ;  $**P < 0.02$ . **C**: INS1 cells were treated as indicated and were labeled with TMRE. Scale bars = 14  $\mu$ m. **D**: Results from the TMRE labeling (shown in **C**) were quantified (mean  $\pm$  SE).  $*P < 0.001$ ;  $**P < 0.0001$ . **E**: Proliferation of INS1 cells was determined through the use of BrdU staining. Data shown are the mean  $\pm$  SE ( $n = 3$  or 4).  $*P < 0.01$ ;  $**P < 0.001$ ;  $***P < 0.0001$ . **F**: Immunoblots from extracts of human islets that were treated as shown. The arrow indicates Keap1. **G**: Dispersed human islets were labeled with MitoTracker Red CMXRos (Mito). Scale bars = 10  $\mu$ m. **H**: Quantification of the staining shown in **G**.  $**P < 0.01$ . **I**: Dispersed human islet cells were fixed and stained for insulin and Ki67. Results are a percentage of Ki67- and insulin-positive cells. Data shown are the mean  $\pm$  SE ( $n = 5$ ).  $*P < 0.05$ ,  $**P < 0.01$ ,  $***P < 0.001$ . arb., arbitrary; Glu, glucose; ins, insulin; MFI, mean fluorescence intensity.

rodent and human  $\beta$ -cell proliferation. Increased Nrf2 abundance was associated with enhanced anabolic activity, including increased anabolic metabolites, increased mitochondrial content and activity, and increased glucose-stimulated proliferation (Fig. 8).

Using loss- and gain-of-function experiments, we showed that ChREBP is required for glucose-stimulated  $\beta$ -cell proliferation and that overexpression of ChREBP amplified the effect of glucose on proliferation, without apparent ill effects (4). We also recently demonstrated that the feed-forward induction of the newly identified ChREBP $\beta$  isoform is necessary for glucose-stimulated  $\beta$ -cell proliferation (11). These

results were surprising in the face of numerous studies implicating ChREBP in glucose toxicity (12,22–24). In the current study, however, direct comparison of ChREBP $\alpha$  and ChREBP $\beta$  overexpression in  $\beta$ -cells demonstrated that apoptosis results when ChREBP $\beta$  is expressed to levels many fold higher than physiological levels, an observation consistent with a previous report (12). By contrast, ChREBP $\alpha$  overexpression in INS1 cells or human islets does not affect GSIS and does not result in apoptosis, observations congruent with those of Wang et al. (13). Together these observations suggest that physiological induction of the potent, constitutively active, nuclear ChREBP $\beta$  isoform is

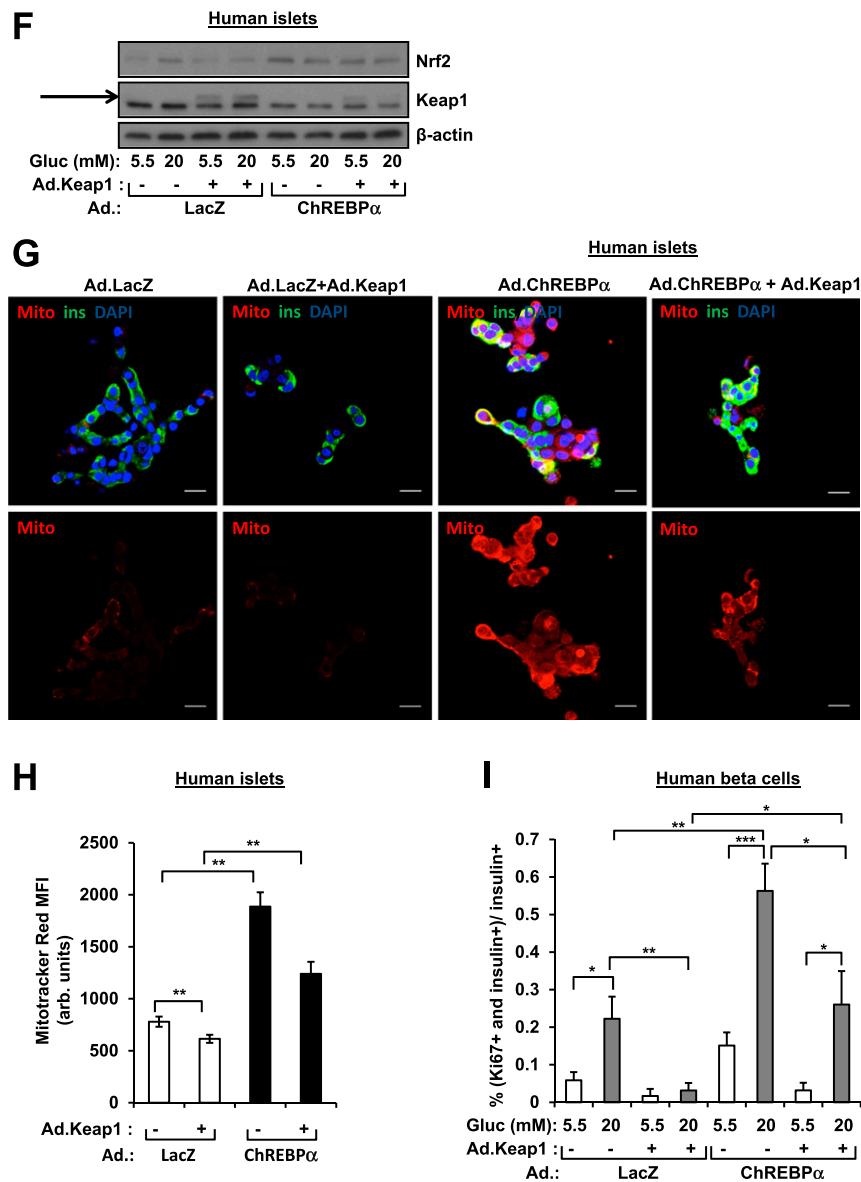
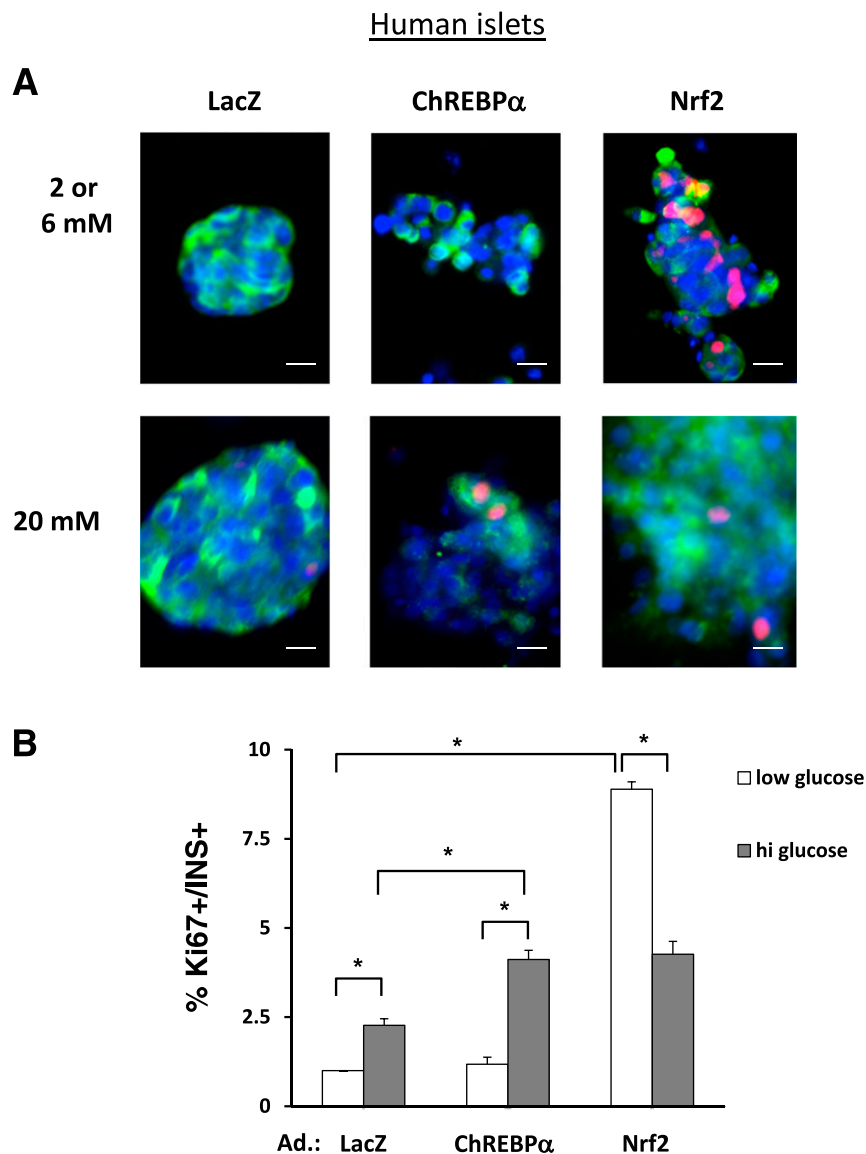


Figure 6—Continued.

necessary for adaptive  $\beta$ -cell expansion, but that too much for too long, as may happen from prolonged hyperglycemia in diabetes (12) or through overexpression with viral vectors, is harmful to  $\beta$ -cells. In addition, because treatment with ChREBP $\alpha$  exerts a positive effect on  $\beta$ -cell anabolism and proliferation, and initiates an antioxidant pathway, therapies that adjust the ratio between ChREBP $\alpha$  and ChREBP $\beta$  may be beneficial to patients with diabetes who have insufficient  $\beta$ -cell mass. It is interesting that Shalev and colleagues (36) found that ChREBP $\beta$  and ChREBP $\alpha$  oppose each other's effects. Those authors demonstrated that ChREBP $\beta$  overexpression decreases ChREBP $\alpha$  abundance, and they postulated that the role of ChREBP $\beta$  is to prevent ChREBP $\alpha$  from mediating glucose toxicity. Those experiments were performed within relatively short time frames and did not assess apoptosis.

Further experiments are needed to resolve these differences and to test the effects of each isoform on the activity of the other with respect to proliferation, apoptosis, and function.

ChREBP $\alpha$  increased Nrf2 in both rodent and human  $\beta$ -cells, providing an explanation for the augmented anabolic response of ChREBP $\alpha$  in the absence of apoptosis. In its basal state, Nrf2 is tightly bound by Keap1, an adaptor protein that brings a Cullin3-Rbx1 E3 ligase complex into close proximity to Nrf2, leading to rapid ubiquitination and degradation of Nrf2 in proteasomes (34,35). Upon alkylation, oxidation, or conformational change, Keap1 has a reduced affinity for Nrf2, relieving its ubiquitination and degradation. Nrf2 is then free to migrate to the nucleus and activate AREs in the regulatory regions of target genes. An important target of Nrf2 is



**Figure 7**—Exogenous Nrf2 is sufficient to drive proliferation of human  $\beta$ -cells. Dispersed human islets were transduced with the indicated adenoviruses for a total of 48 h. Cells were cultured in either 2 or 6 mmol/L glucose (low glucose) or 20 mmol/L glucose (high glucose). The high glucose was added for the last 16 h of the experiment. **A**: Cells were fixed and immunostained for insulin and Ki67; these results are quantified in **B**. Scale bars = 40  $\mu$ m. Data are the mean  $\pm$  SE of the percentage of cells that were both Ki67- and insulin (INS)-positive ( $n = 6$ ). \* $P < 0.05$ .

Nrf1, which—along with PGC family members—activates AREs that drive mitochondrial biogenesis (37). Other important targets of Nrf2 include antioxidant enzymes such as heme oxygenase-1, NAD(P)H dehydrogenase, and quinone 1, and induction of these enzymes is closely associated with the role of Nrf2 in protection against oxidative stress (31). Chromatin immunoprecipitation sequencing studies have identified hundreds of Nrf2 gene targets (38,39). In addition to antioxidant genes, these include numerous genes involved in intermediary metabolism, including the pentose phosphate pathway, providing reducing equivalents that are useful for antioxidant enzymes and are building blocks for proliferation (32,33).

It follows that Nrf2 also promotes increased mitochondrial function (30).

To our knowledge, this study is the first to demonstrate that Nrf2 is required for glucose-stimulated  $\beta$ -cell proliferation and, when overexpressed, is sufficient to drive human  $\beta$ -cell proliferation. The role of Nrf2 in  $\beta$ -cells has only recently been explored, and research has been largely restricted to its antioxidant properties. Abebe et al. (40) recently found that female Zucker fatty rats recovering from a short-term high-fat diet have  $\beta$ -cell function and morphology largely restored through the Nrf2 pathway. Furthermore, Uruno et al. (41), using a global Keap1<sup>+/-</sup> knockout mouse on a db/db genetic background,

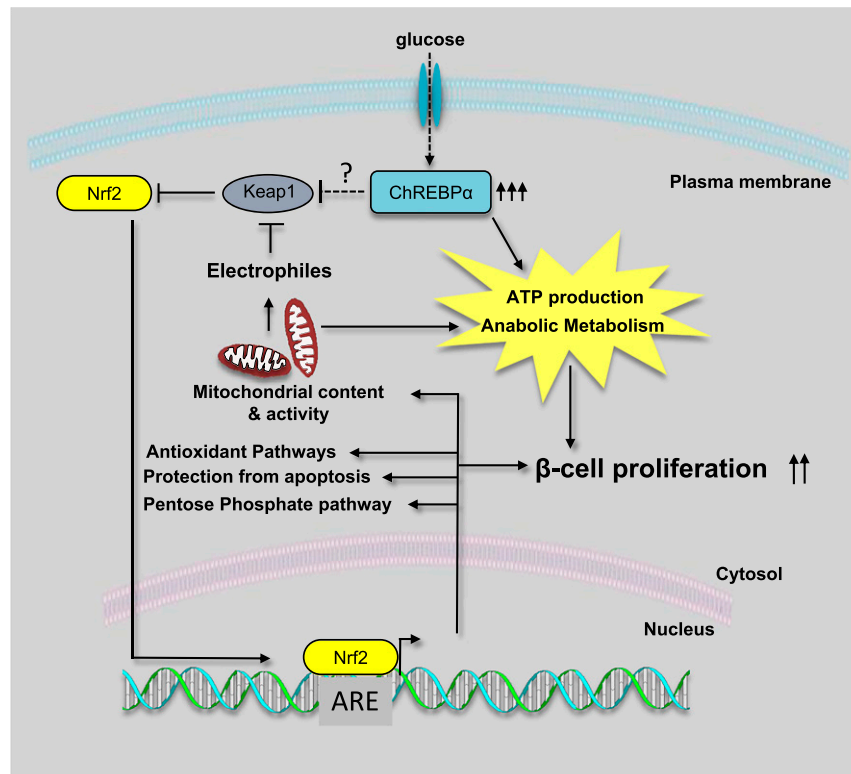


**Figure 8**—Model of ChREBP $\alpha$ -mediated activation of the Nrf2 and anabolic pathways driving  $\beta$ -cell proliferation. ChREBP $\alpha$  inhibits Keap1 activity, contributing to an increase in Nrf2 abundance. Nrf2 binds to AREs, which drives expression of antioxidant and metabolic enzyme genes. Mitochondrial biogenesis and activity increase, resulting in increased ATP production and anabolic metabolism. A potential feedback loop contributes to the maintenance of the anabolic state, whereby electrophiles inhibit Keap1-Nrf2 interaction through the disruption of cysteine residues. Increased ATP production and anabolic metabolism contribute to increased glucose-stimulated  $\beta$ -cell proliferation.

demonstrated that activation of the Nrf2 pathway prevented diabetes, in part by preserving  $\beta$ -cell mass. Yagishita et al. (42) demonstrated that activation of Nrf2 protects  $\beta$ -cells from the stress of inducible nitric oxide synthase overexpression in mice. Masuda et al. (43) transplanted human islets into mice after treatment with an Nrf2 activator. Unfortunately, that study only examined the proportion of mice rescued from hyperglycemia after islet transplantation and found no difference from the controls. That study did not test rates of human  $\beta$ -cell survival immediately after transplantation into euglycemic or diabetic mice. The same group found that Nrf2 activation improved rat islet transplantation outcomes (44), but the same analysis has not been done with human islets. Horn et al. (45), using a bioinformatics approach, identified Nrf2 among a set of transcription factors that mediate adaptive expansion of  $\beta$ -cell mass, including Myc, Mycn, Hnf1 $\alpha$ , Hnf4 $\alpha$ , and E2f1. How might Nrf2 mediate  $\beta$ -cell proliferation? Nrf2 activates antioxidant genes as well as genes of the pentose phosphate pathway, presumably in order to generate NADPH to restore antioxidant enzyme redox balance (14). In addition, NADPH is an important reducing equivalent for lipogenesis and DNA synthesis, which are crucial for proliferating cells (25). Thus, activation of Nrf2 may serve a dual role in  $\beta$ -cell

proliferation: as an inducer of antioxidant enzymes and in support of the anabolic production of biomass before cytokinesis.

Balancing ROS production with protection against ROS may be critical for  $\beta$ -cell function and survival. Some ROS are necessary for maximal GSIS in  $\beta$ -cells (46,47). Thus, it has been argued that increasing Nrf2 in  $\beta$ -cells, associated with increased antioxidant activity, may inhibit the ROS production that supports GSIS (48). In the current study, however, we found that ChREBP distinctly imparts antioxidant effects via Nrf2 without affecting GSIS (Supplementary Fig. 2E). It is important to note that our observations show that induction of Nrf2 is not a result of oxidative or endoplasmic reticulum stress, because the classic stress markers Atf3 and C/EBP homologous protein were not induced in ChREBP $\alpha$ -treated  $\beta$ -cells. We also found that ChREBP $\alpha$  does not alter ROS levels (Supplementary Fig. 8). Thus, in our study, ChREBP $\alpha$  increased mitochondrial and anabolic activities, with their attendant increase in ROS production, but this is countered by activation of Nrf2 and increased antioxidant enzyme production.

Keap1 and Nrf2 interact with each other and with other proteins. One important interaction that might at least partly explain our results is the interaction between Keap1

and p62, the regulator of autophagy (49). Activation of autophagy or mitophagy might stimulate mitochondrial biogenesis. Therefore, we tested whether overexpression of ChREBP $\alpha$  or Nrf2 activated autophagy (Supplementary Fig. 9). Glucose, ChREBP $\alpha$ , and Nrf2 all decreased autophagosome labeling. Furthermore, the expression of autophagy genes generally decreased, with the exception of *Ulk1*, which was increased in response to Nrf2. Thus, ChREBP $\alpha$  does not activate autophagy, but further experiments should be performed to clarify how Nrf2 overexpression interacts with autophagy pathways.

A limitation of our study is that we did not identify the mechanism(s) through which ChREBP $\alpha$  inhibits Keap1. Attempts at coimmunoprecipitation of ChREBP $\alpha$  and Keap1 were unsuccessful (data not shown). Another limitation of our study is that the metabolic analysis was cross-sectional. While our results are consistent with those from an anabolic cell that is primed for proliferation, a more longitudinal approach or one that uses isotopomeric substrates to analyze changes in metabolic fluxes as the cells transition from a quiescent to a proliferative state would be more revealing. Future studies will focus on the precise molecular mechanisms through which ChREBP $\alpha$  and Nrf2 alter  $\beta$ -cell metabolism and phenotype.

In summary, we explored the mechanisms through which ChREBP $\alpha$  amplifies glucose-stimulated proliferation of rodent and human  $\beta$ -cells. We found that ChREBP $\alpha$  reduces Keap1 abundance, activating Nrf2, a transcription factor that initiates genetic programs of antioxidant protection, mitochondrial biogenesis, and anabolic metabolism. We found that the induction of Nrf2 was required for normal and for ChREBP $\alpha$ -augmented  $\beta$ -cell proliferation. Dissecting ChREBP $\alpha$ - and Nrf2-driven anabolic pathways should provide new opportunities for designing  $\beta$ -cell regenerative therapies.

**Acknowledgments.** The authors thank Dr. Howard Towle (University of Minnesota) for the ChREBP $\alpha$ -expressing adenovirus and Dr. Chris Newgard (Stedman Nutrition and Metabolism Center, Duke University) for providing INS1-derived 832/13 cells and for helpful discussions. The authors thank Dr. Andrew Stewart (Icahn School of Medicine at Mount Sinai, New York, NY) for helpful discussions and Gabrielle Brill (Icahn School of Medicine at Mount Sinai, New York, NY) for providing technical assistance. The authors also thank the Icahn School of Medicine at Mount Sinai Microscopy Core, the Albert Einstein School of Medicine Stable Isotope & Metabolomics Core, and the Einstein/Sinai Diabetes Center Human Islet and Adenovirus Core.

**Funding.** This work was supported by Deutsche Forschungsgemeinschaft (grant no. DFG SCHU 3023/1-1 to A.M.S.), the National Institute of Diabetes and Digestive and Kidney Diseases (grant nos. T32 DK007516 to M.K., P30 DK020541-38 to A.G.-O., R01 DK100425 to M.A.H., and R01 DK065149 and R01 DK108905 to D.K.S.), the National Institute on Aging (grant no. R01 AG047182 to C.M.H.), the National Cancer Institute (grant no. R01 CA206005 to J.E.C.), the National Institute of Allergy and Infectious Diseases (grant no. R01 AI093637 to D.H.), the American Diabetes Association (grant nos. ADA 7-11-BS-128 and ADA 1-17-IBS-116 to D.K.S.), and JDRF (grant no. SRF 17-2011-598 to D.K.S.). J.E.C. has received an American Cancer Society Research Scholar Award.

**Duality of Interest.** No potential conflicts of interest relevant to this article were reported.

**Author Contributions.** A.K., L.S.K., A.M.S., M.K., L.B.H., B.D., and L.L. performed the investigation. A.K., L.S.K., A.M.S., A.G.-O., M.A.H., C.M.H., J.E.C., and D.K.S. wrote, reviewed, and edited the manuscript. A.K. and D.K.S. conceptualized the study and wrote the first draft of the manuscript. A.G.-O., M.A.H., C.M.H., J.E.C., D.H., and D.K.S. acquired funding. M.K., M.A.H., C.M.H., and D.K.S. provided resources. A.G.-O., M.A.H., C.M.H., J.E.C., D.H., and D.K.S. supervised the study. D.K.S. is the guarantor of this work and, as such, had full access to all the data in the study and takes responsibility for the integrity of the data and the accuracy of the data analysis.

**Prior Presentation.** Some data were presented at the 77th Scientific Sessions of the American Diabetes Association, San Diego, CA, 9–13 June 2017.

## References

- Wang P, Alvarez-Perez JC, Felsenfeld DP, et al. A high-throughput chemical screen reveals that harmine-mediated inhibition of DYRK1A increases human pancreatic beta cell replication. *Nat Med* 2015;21:383–388
- Alonso LC, Yokoe T, Zhang P, et al. Glucose infusion in mice: a new model to induce beta-cell replication. *Diabetes* 2007;56:1792–1801
- Bonner-Weir S, Deery D, Leahy JL, Weir GC. Compensatory growth of pancreatic beta-cells in adult rats after short-term glucose infusion. *Diabetes* 1989;38:49–53
- Metukuri MR, Zhang P, Basantani MK, et al. ChREBP mediates glucose-stimulated pancreatic  $\beta$ -cell proliferation. *Diabetes* 2012;61:2004–2015
- Porat S, Weinberg-Corem N, Tornovsky-Babaey S, et al. Control of pancreatic  $\beta$  cell regeneration by glucose metabolism. *Cell Metab* 2011;13:440–449
- Wang P, Fiaschi-Taesch NM, Vasavada RC, Scott DK, García-Ocaña A, Stewart AF. Diabetes mellitus—advances and challenges in human  $\beta$ -cell proliferation. *Nat Rev Endocrinol* 2015;11:201–212
- Levitt HE, Cyphert TJ, Pascoe JL, et al. Glucose stimulates human beta cell replication in vivo in islets transplanted into NOD-severe combined immunodeficiency (SCID) mice. *Diabetologia* 2011;54:572–582
- Postic C, Dentin R, Denechaud PD, Girard J. ChREBP, a transcriptional regulator of glucose and lipid metabolism. *Annu Rev Nutr* 2007;27:179–192
- Filhoulaud G, Guilmeau S, Dentin R, Girard J, Postic C. Novel insights into ChREBP regulation and function. *Trends Endocrinol Metab* 2013;24:257–268
- Herman MA, Peroni OD, Villoria J, et al. A novel ChREBP isoform in adipose tissue regulates systemic glucose metabolism. *Nature* 2012;484:333–338
- Zhang P, Kumar A, Katz LS, et al. Induction of the ChREBP $\beta$  isoform is essential for glucose-stimulated  $\beta$ -cell proliferation. *Diabetes* 2015;64:4158–4170
- Poungvarin N, Lee JK, Yechoor VK, et al. Carbohydrate response element-binding protein (ChREBP) plays a pivotal role in beta cell glucotoxicity. *Diabetologia* 2012;55:1783–1796
- Wang H, Kouri G, Wollheim CB. ER stress and SREBP-1 activation are implicated in beta-cell glucolipotoxicity. *J Cell Sci* 2005;118:3905–3915
- Ma Q, He X. Molecular basis of electrophilic and oxidative defense: promises and perils of Nrf2. *Pharmacol Rev* 2012;64:1055–1081
- Urano A, Yagishita Y, Yamamoto M. The Keap1-Nrf2 system and diabetes mellitus. *Arch Biochem Biophys* 2015;566:76–84
- Gao B, Doan A, Hybertson BM. The clinical potential of influencing Nrf2 signaling in degenerative and immunological disorders. *Clin Pharmacol* 2014;6:19–34
- Hohmeier HE, Mulder H, Chen G, Henkel-Rieger R, Prentki M, Newgard CB. Isolation of INS-1-derived cell lines with robust ATP-sensitive K<sup>+</sup> channel-dependent and -independent glucose-stimulated insulin secretion. *Diabetes* 2000;49:424–430
- Zhang P, Metukuri MR, Bindom SM, Prochownik EV, O'Doherty RM, Scott DK. c-Myc is required for the ChREBP-dependent activation of glucose-responsive genes. *Mol Endocrinol* 2010;24:1274–1286
- Kumar A, Harris TE, Keller SR, Choi KM, Magnuson MA, Lawrence JC Jr. Muscle-specific deletion of rictor impairs insulin-stimulated glucose transport and enhances basal glycogen synthase activity. *Mol Cell Biol* 2008;28:61–70

20. Serasinghe MN, Wieder SY, Renault TT, et al. Mitochondrial division is requisite to RAS-induced transformation and targeted by oncogenic MAPK pathway inhibitors. *Mol Cell* 2015;57:521–536
21. García-Ocaña A, Vasavada RC, Cebrian A, et al. Transgenic overexpression of hepatocyte growth factor in the beta-cell markedly improves islet function and islet transplant outcomes in mice. *Diabetes* 2001;50:2752–2762
22. Cha-Molstad H, Saxena G, Chen J, Shalev A. Glucose-stimulated expression of Txnip is mediated by carbohydrate response element-binding protein, p300, and histone H4 acetylation in pancreatic beta cells. *J Biol Chem* 2009;284:16898–16905
23. Chen J, Fontes G, Saxena G, Poitout V, Shalev A. Lack of TXNIP protects against mitochondria-mediated apoptosis but not against fatty acid-induced ER stress-mediated beta-cell death. *Diabetes* 2010;59:440–447
24. da Silva Xavier G, Rutter GA, Diraison F, Andreolas C, Leclerc I. ChREBP binding to fatty acid synthase and L-type pyruvate kinase genes is stimulated by glucose in pancreatic beta-cells. *J Lipid Res* 2006;47:2482–2491
25. Vander Heiden MG, Cantley LC, Thompson CB. Understanding the Warburg effect: the metabolic requirements of cell proliferation. *Science* 2009;324:1029–1033
26. Marelli-Berg FM, Fu H, Mauro C. Molecular mechanisms of metabolic reprogramming in proliferating cells: implications for T-cell-mediated immunity. *Immunology* 2012;136:363–369
27. Scaduto RC Jr, Grotyohann LW. Measurement of mitochondrial membrane potential using fluorescent rhodamine derivatives. *Biophys J* 1999;76:469–477
28. Liesa M, Shirihai OS. Mitochondrial dynamics in the regulation of nutrient utilization and energy expenditure. *Cell Metab* 2013;17:491–506
29. Pendergrass W, Wolf N, Poot M. Efficacy of MitoTracker Green and CMXRosamine to measure changes in mitochondrial membrane potentials in living cells and tissues. *Cytometry A* 2004;61:162–169
30. Holmström KM, Baird L, Zhang Y, et al. Nrf2 impacts cellular bioenergetics by controlling substrate availability for mitochondrial respiration. *Biol Open* 2013;2:761–770
31. Itoh K, Ye P, Matsumiya T, Tanji K, Ozaki T. Emerging functional cross-talk between the Keap1-Nrf2 system and mitochondria. *J Clin Biochem Nutr* 2015;56:91–97
32. Mitsuishi Y, Taguchi K, Kawatani Y, et al. Nrf2 redirects glucose and glutamine into anabolic pathways in metabolic reprogramming. *Cancer Cell* 2012;22:66–79
33. Hayes JD, Dinkova-Kostova AT. The Nrf2 regulatory network provides an interface between redox and intermediary metabolism. *Trends Biochem Sci* 2014;39:199–218
34. Cullinan SB, Gordan JD, Jin J, Harper JW, Diehl JA. The Keap1-BTB protein is an adaptor that bridges Nrf2 to a Cul3-based E3 ligase: oxidative stress sensing by a Cul3-Keap1 ligase. *Mol Cell Biol* 2004;24:8477–8486
35. Kobayashi A, Kang MI, Okawa H, et al. Oxidative stress sensor Keap1 functions as an adaptor for Cul3-based E3 ligase to regulate proteasomal degradation of Nrf2. *Mol Cell Biol* 2004;24:7130–7139
36. Jing G, Chen J, Xu G, Shalev A. Islet ChREBP- $\beta$  is increased in diabetes and controls ChREBP- $\alpha$  and glucose-induced gene expression via a negative feedback loop. *Mol Metab* 2016;5:1208–1215
37. Piantadosi CA, Carraway MS, Babiker A, Suliman HB. Heme oxygenase-1 regulates cardiac mitochondrial biogenesis via Nrf2-mediated transcriptional control of nuclear respiratory factor-1. *Circ Res* 2008;103:1232–1240
38. Chorley BN, Campbell MR, Wang X, et al. Identification of novel NRF2-regulated genes by ChIP-Seq: influence on retinoid X receptor alpha. *Nucleic Acids Res* 2012;40:7416–7429
39. Malhotra D, Portales-Casamar E, Singh A, et al. Global mapping of binding sites for Nrf2 identifies novel targets in cell survival response through ChIP-seq profiling and network analysis. *Nucleic Acids Res* 2010;38:5718–5734
40. Abebe T, Mahadevan J, Bogachus L, et al. Nrf2/antioxidant pathway mediates  $\beta$  cell self-repair after damage by high-fat diet-induced oxidative stress. *JCI Insight* 2017;2. pii: 92854
41. Uruno A, Furusawa Y, Yagishita Y, et al. The Keap1-Nrf2 system prevents onset of diabetes mellitus. *Mol Cell Biol* 2013;33:2996–3010
42. Yagishita Y, Fukutomi T, Sugawara A, et al. Nrf2 protects pancreatic  $\beta$ -cells from oxidative and nitrosative stress in diabetic model mice. *Diabetes* 2014;63:605–618
43. Masuda Y, Vaziri ND, Li S, et al. The effect of Nrf2 pathway activation on human pancreatic islet cells. *PLoS One* 2015;10:e0131012
44. Li S, Vaziri ND, Masuda Y, et al. Pharmacological activation of Nrf2 pathway improves pancreatic islet isolation and transplantation. *Cell Transplant* 2015;24:2273–2283
45. Horn S, Kirkegaard JS, Hoelper S, et al. Research resource: a dual proteomic approach identifies regulated islet proteins during  $\beta$ -cell mass expansion in vivo. *Mol Endocrinol* 2016;30:133–143
46. Pi J, Bai Y, Zhang Q, et al. Reactive oxygen species as a signal in glucose-stimulated insulin secretion. *Diabetes* 2007;56:1783–1791
47. Leloup C, Tourrel-Cuzin C, Magnan C, et al. Mitochondrial reactive oxygen species are obligatory signals for glucose-induced insulin secretion. *Diabetes* 2009;58:673–681
48. Pi J, Zhang Q, Fu J, et al. ROS signaling, oxidative stress and Nrf2 in pancreatic beta-cell function. *Toxicol Appl Pharmacol* 2010;244:77–83
49. Komatsu M, Kurokawa H, Waguri S, et al. The selective autophagy substrate p62 activates the stress responsive transcription factor Nrf2 through inactivation of Keap1. *Nat Cell Biol* 2010;12:213–223